

UC San Diego

UC San Diego Previously Published Works

Title

The evolution of radiation-dominated stars. I - Nonrotating supermassive stars

Permalink

<https://escholarship.org/uc/item/8921z0pt>

Journal

The Astrophysical Journal, 307(2)

ISSN

0004-637X

Authors

Fuller, GM
Woosley, SE
Weaver, TA

Publication Date

1986-08-01

DOI

10.1086/164452

Peer reviewed

THE EVOLUTION OF RADIATION-DOMINATED STARS. I. NONROTATING SUPERMASSIVE STARS¹

G. M. FULLER AND S. E. WOOSLEY

Board of Studies in Astronomy and Astrophysics, Lick Observatory, University of California, and
 Special Studies Group, Lawrence Livermore National Laboratory

AND

T. A. WEAVER

Special Studies Group and R-Program, Lawrence Livermore National Laboratory

Received 1985 July 11; accepted 1986 February 5

ABSTRACT

The evolution of nonrotating supermassive stars ($M \gtrsim 5 \times 10^4 M_\odot$) is examined in detail using the results of hydrodynamic calculations which include post-Newtonian approximations to general relativistic gravity, an equation of state which includes electron-positron pairs, and all relevant nuclear reactions. These calculations are followed through the period of quasi-static contraction, the general relativistic instability, and the eventual collapse to a black hole or disruption via a thermonuclear explosion. It is found that stars with mass $M \gtrsim 10^5 M_\odot$ and initial metallicities $Z \lesssim 0.005$ do not explode. The objects with $Z \gtrsim 0.005$ do explode because of the burning of hydrogen by the β -limited CNO cycle. Explosion energies range from 2.0×10^{56} ergs for stars of mass $M \approx 10^5 M_\odot$ to 2.5×10^{57} ergs for $M \approx 10^6 M_\odot$. For those stars that do not explode the collapse to a black hole is found to be nonhomologous.

Subject headings: stars: evolution — stars: interiors — stars: massive

I. INTRODUCTION

This is the first in a series of papers examining the evolution of stars close to instability where electron-positron pair creation, post-Newtonian corrections to gravity, or other normally negligible effects may have a profound influence on the evolution. This paper will treat the evolution of nonrotating supermassive stars. Subsequent papers in this series will address the evolution of *rotating* supermassive stars, nonrotating very massive stars, and post-Newtonian effects in pre-supernova stars ($10 \lesssim M/M_\odot \lesssim 100$). *Very massive* stars (VMOs) are defined here to be stars so massive that at some point in their evolution they collapse on an electron-positron pair instability. This corresponds to stars more massive than $\sim 100 M_\odot$ but less than $5 \times 10^4 M_\odot$ (Bond, Arnett, and Carr 1984; Woosley and Weaver 1982; Zeldovich and Novikov 1971). Stars still more massive than this will first collapse on the general relativistic gravitational instability before igniting hydrogen burning (Hoyle and Fowler 1963; Feynman 1963; Chandrasekhar 1964; Iben 1963), and we hereafter follow Fowler and Hoyle (1964) and designate these objects as *super-massive* stars (SMOs).

We specialize our discussion in this paper to the classic problem of the evolution of supermassive stars (Fowler 1964; Iben 1963): given that such an object has formed and has quasi-statically contracted to the point of dynamical instability because of the small effects of general relativity, is the nuclear energy liberated in the subsequent collapse enough to blow up the star? Concomitantly we would like to know the grid of initial masses and metallicities which results in explosions and the characteristics of the nucleosynthesis produced. The explosions themselves may be important for galaxy formation models such as those of Ostriker and Cowie (1981). This work is in the spirit of the pioneering survey carried out by Fricke

(1973, 1974) and Appenzeller and Fricke (1972). The problem warrants reinvestigation, however, because of our increased understanding of the nuclear physics of hot hydrogen burning (Wallace and Woosley 1981; Wiescher 1984) and the need to attack an essentially hydrodynamic problem with a numerical hydrodynamics computer code employing an exact equation of state which includes electron-positron pairs and all sources of neutrino (antineutrino) emission.

II. GENERAL COMMENTS ON SUPERMASSIVE STARS

The large amounts of energy emission from the giant radio sources, and later the discovery of the QSO (Schmidt 1963), stimulated the first interest in supermassive stars. If the quasi-stellar sources are at cosmological distances, their absolute luminosities are very large: 10^{44} – 10^{46} ergs s^{-1} . Hoyle and Fowler (1963) proposed that supermassive $n = 3$ polytropes would account for the large energy budget of the giant radio sources. However, it was found that the post-Newtonian instability would cause the supermassive star to become dynamically unstable during hydrogen burning (Iben 1963). This limits the lifetime of the star to the quasi-static contraction phase prior to hydrogen ignition which is, as we will discuss, only a few thousand years for stars of mass in the range of 10^5 – $10^6 M_\odot$. It is known that the lifetime of the active phenomena associated with QSOs and giant radio sources can be of order 10^8 yr. This follows from the special nature of the giant radio sources (Fowler 1965), which are known to maintain a beam of relativistic particles from the central object to the radio lobes for times of order 10^8 yr. This lifetime constraint led Salpeter (1964) to suggest that accretion on a supermassive blackhole was the central engine of the QSO phenomenon and there is growing evidence that this is indeed the correct picture (Blandford 1984). However, Stoner and Ptak (1984) have recently suggested that $10^6 M_\odot$ supermassive stars may be the central engines of some Seyfert galaxies showing variability in their *IUE* spectra.

¹ Lick Observatory Bulletin, No. B1042.

Even if supermassive black holes do provide the energy source for QSOs the evolutionary scenario leading to their origin remains to be determined. This problem has received scant attention because of the inherent uncertainties, yet the general picture is one of collapse and coalescence of massive clusters of stars near galactic centers. The work of Begelman and Rees (1978) provides a scenario for the evolution of a densely populated galactic core. Along one path of their evolutionary flow chart, a dense cluster of $1 M_{\odot}$ main-sequence stars undergoes coalescence and disruptive collisions to form an amorphous massive gas cloud of mass between 10^5 and $10^8 M_{\odot}$ which then falls to the center to establish a brief phase of hydrostatic equilibrium. Such a supermassive star will suffer a post-Newtonian instability leading to one of several possibilities: a nuclear explosion, bifurcation into a binary with copious gravitational radiation and collapse to a black hole; fragmentation into three or more objects with the possible ejection of one; or simply ordered collapse to a "seed" black hole on which further accretion of stellar material will build the central engine of an active galactic nucleus. As we shall see in the next section, the entropy per baryon in a supermassive star in hydrostatic equilibrium is of order 100 times that of a typical main-sequence star (Shapiro and Teukolsky 1983). This suggests that the formation process for such an object is highly dissipative, like that involved in a process of stellar collisions, disruption, and coalescence. Sanders (1970) has also discussed the coalescence of a large star cluster into a supermassive star.

Considerable work has also gone into investigating rotating magnetized supermassive stars as the central engines in active galactic nuclei (Ozernoy and Usov 1971; Fowler 1966). These objects can avoid many of the lifetime constraints associated with nonrotating stars. Such *spinars* will not be considered in this paper.

Another arena in which the possibility of supermassive objects arise is the early universe, specifically, as a constituent in a possible first generation of stars or Population III. There are several reasons for considering the existence of supermassive stars in such an early, low-metallicity environment. The first of these is that star formation in the absence of cooling agents such as metals and grains may be quite different than in standard star-formation processes, resulting in an initial mass function skewed toward higher masses (Silk 1977; but see also Palla, Salpeter, and Stahler 1983). Second there is nucleosynthetic evidence of an early generation of stars that provided a burst of nucleosynthesis consistent with an initial mass function peaked toward heavier stars (Truran and Cameron 1971). Finally the existence of isothermal fluctuations of order $10^6 M_{\odot}$ suggests that very massive and supermassive star progenitor clouds may have had density enhancements in the nonlinear growth regime at decoupling (Dicke and Peebles 1968).

Star formation theories suggest that a low-metallicity environment may be associated with low cooling rates in collapsing protostellar clouds which, in turn, may delay or suppress fragmentation in these clouds. Larson and Starrfield (1971) have argued that an upper mass limit on star formation processes comes when the Kelvin-Helmholtz time of the core of the cloud, or protostar, is less than the time for accretion of more material. With roughly solar abundances and at $T \approx 20$ K for an initial cloud the upper mass limit is near $60 M_{\odot}$, but other authors have found increased upper limits of the mass spectrum, including Yoneyama (1972) ($M_{\max} \approx 10^2$ – $10^4 M_{\odot}$) and Tohlin (1980) ($M_{\max} \gtrsim 200 M_{\odot}$). All of these studies may

arrive at erroneous conclusions because of an incorrect assessment of the cooling effect of molecular hydrogen (Lepp and Shull 1984). If this is the case, these same studies can be used to show that formation of VMO and SMO protostars in the conventional manner is unlikely.

It has been pointed out that even should a star of $M \gtrsim 60 M_{\odot}$ form it would be unstable to nuclear-burning driven pulsations (Ledoux 1941). This is the frequently cited reason why stars in the $M \gtrsim 100 M_{\odot}$ range are not observed. However, later work (Talbot 1971), which includes nonlinear hydrodynamic effects, suggests that these pulsations may be damped to finite amplitudes. Pulsations of this nature were observed in our calculations although in fact no quantitative conclusions can be drawn because of the damping nature of the implicit hydrodynamics scheme employed.

Despite these arguments against the formation of VMOs and SMOs in the conventionally accepted manner of star formation there is observational evidence which suggests that star formation was quantitatively and qualitatively different in the past. There is the observation that there are very few zero metallicity dwarf stars observed: the "G-dwarf problem." Almost all stars of extreme age seem to have some heavy element enrichment. Models of galactic chemical evolution suggest a burst of initial metal enrichment (Truran and Cameron 1971). Evidence that massive stars are to be implicated in this enrichment process comes from the "oxygen anomaly:" the observation that the oxygen to iron ratio is ~ 3 times the solar value for stars with low iron abundances; whereas stars with higher iron abundance show a lower oxygen to iron ratio. Since oxygen is preferentially synthesized over iron in higher mass stars the conclusion is that there must have been an early generation of massive stars. This argument says nothing about the upper mass limit of this Population III generation, only that there was a higher proportion of massive stars.

There is direct observational evidence, although still controversial, for the existence of a $500 M_{\odot}$ – $2200 M_{\odot}$ object in the Doradus feature of the LMC (Cassinelli *et al.* 1981). The evidence relies on speckle interferometry data, observations of variability, an observed wind, and, of course, the volume of ionized hydrogen. Some of the data are consistent with interpretation of the object as a tight association of normal massive O and B stars, although most of the data are not. We refer the reader to Bond, Arnett, and Carr (1984) for a complete discussion of the VMO question. If this object is indeed a VMO then it calls into question the above picture of star formation. If there can be $2200 M_{\odot}$ stars then perhaps there can be $10^5 M_{\odot}$ stars.

There also exists indirect evidence for the past explosion of very massive objects. Notably supernova 1961 V (Branch and Greenstein 1971; Chevalier 1981; Branch 1984) that had roughly a type I supernova light curve, but an aberrant luminosity and spectrum that has been interpreted by Utroba (1984) as the explosion of a $2000 M_{\odot}$ star.

One way to address that question is to derive the expected characteristics of the evolution, collapse, explosion and nucleosynthesis of supermassive stars, so as to put constraints on formation sites and the role they may or may not have played in galactic evolution. There have been many attempts to derive the structure and evolution of supermassive stars and most of them have addressed the central question of explosion-collapse stated at the outset of this introduction. In addition to the work of Hoyle and Fowler (1963) and Fowler (1964), there has

been a series of papers centering around the thermonuclear evolution of supermassive stars. Bisnovatyi-Kogan (1968) found that nuclear explosions were the end result of the evolution of stars in the 6×10^4 – $1.5 \times 10^5 M_\odot$ range. Fricke (1973, 1974) and Apenzeller and Fricke (1972) performed a survey of supermassive star evolution using averaged polytropic configurations and hydrodynamic calculations, and taking account of the limit on the CNO burning rate imposed by the β^+ decay lifetimes of ^{14}O and ^{15}O (the β -limited CNO rate; Fowler 1965) found that stars in the mass range 10^5 – $10^6 M_\odot$ and initially zero metallicity collapsed to black holes. Stars of higher metallicity were found to explode. Norgaard and Fricke (1976) pointed out the important role of the β -limit in limiting the range of exploding masses and metallicities of supermassive stars.

Wallace and Woosley (1981) elucidated the nuclear physics of the rp-process: the rapid proton capture process that characterizes hydrogen burning at very high temperature ($T_9 > 1$). They found that the energy generation rate in hot hydrogen burning could be 200 or 300 times larger than in the β -limited CNO cycle. This led to speculation that zero metallicity 10^5 – $10^6 M_\odot$ stars might be candidates for explosion and primordial nucleosynthesis after all. Fricke and Ober (1980) reported just such a result using a hydrodynamics computer code and including the rp-process.

Criticisms of previous work have revolved around completeness. Here we attempt to integrate a hydrodynamics calculation with a detailed equation of state including electron-positron pairs, all nuclear reaction rates including the rp-process and neutrino loss processes. We have run a grid of initial masses and metallicities, starting each calculation as a low-density hydrostatic configuration and evolving it quasi-statically to the general relativistic instability point, where the subsequent dynamic evolution is studied in detail, including the nucleosynthesis.

The evolution of supermassive stars is difficult to follow because these stars are always close to $\Gamma_1 \approx 4/3$ and instability. The result is that second-order effects in normal stellar evolution like turbulent pressure, small amounts of rotation, or general relativity become of paramount importance for stability in the radiation-dominated supermassive stars.

III. STABILITY OF RADIATION DOMINATED STARS

As the mass of a star increases, hydrostatic equilibrium demands increasing central temperature, and hence a larger share of the pressure support must be carried by radiation. For an index $n = 3$ polytrope the ratio of gas pressure P_g to the total pressure $P_{\text{tot}} = P_r + P_{\text{gas}}$ can be shown to be (Fowler and Hoyle 1966)

$$\beta = \frac{P_g}{P_{\text{tot}}} \approx \frac{4.3}{\mu} \left(\frac{M_\odot}{M} \right)^{1/2} \approx 10^{-2} \quad \text{for } M \approx 10^6 M_\odot, \quad (1)$$

where μ is the mean molecular weight. Clearly, for supermassive stars in the $M = 10^5$ – $10^6 M_\odot$ range, gas pressure is a minor perturbation on the total pressure of the star. For a star in which radiation pressure is a constant fraction of the total pressure (a good approximation wherever $P_r \gg P_g$) it can be shown that the pressure is,

$$P = \left[\left(\frac{N_A k}{\mu} \right)^4 \frac{3}{a} \frac{(1-\beta)}{\beta^4} \right]^{1/3} \rho^{4/3} \equiv K \rho^{4/3}, \quad (2)$$

where N_A is Avagadro's number, k is Boltzmann's constant, and a is the Stephan-Boltzmann radiation constant. In other words, the star is an index $n = 3$ polytrope.

Where radiation pressure dominates and the polytropic index is near $n = 3$ the temperature gradient is very nearly equal to the adiabatic gradient. The star is thus nearly always unstable to convection in the presence of even a small amount of nuclear burning. There must, however, be a surface radiative zone, where radiation pressure dominates so that $P \approx \frac{1}{3} a T^4$, and the opacity is by electron scattering, $\kappa \approx \sigma/m$, with σ the Thompson scattering cross section and m is the mass of the nucleon. The luminosity must then be nearly Eddington where, for solar abundances,

$$L_{\text{Ed}} \approx 1.3 \times 10^{38} \left(\frac{M}{M_\odot} \right) \text{ ergs s}^{-1} \quad (3)$$

(Shapiro and Teukolsky 1983).

Since the bulk of the star is expected to be convective the entropy will be roughly constant. For stars in which the specific entropy is nearly constant the adiabatic polytropic constant Γ is approximately equal to the local adiabatic index Γ_1 (Chandrasekhar 1939):

$$\Gamma \equiv 1 + \frac{1}{n} \approx \Gamma_1 \equiv \left(\frac{d \ln P}{d \ln \rho} \right)_s. \quad (4)$$

This need not always hold true as, for example, in the case of a massive presupernova red supergiant, where steep entropy ledges exist.

Following Wagoner (1969), Bond *et al.* (1984), Carr, Bond, and Arnett (1981), and Bethe *et al.* (1979) it is instructive to examine the entropy per baryon in supermassive stars. In general, the entropy per unit volume will be the sum of several components,

$$S = S_\gamma + S_{\text{nucleons}} + S_{\text{nuclei}} + S_e, \quad (5)$$

where S_γ is the photon entropy, S_{nucleons} is that due to free neutrons and protons, S_{nuclei} is that due to the ions, and S_e is the electron entropy. The general nonrelativistic expression for the electron entropy per baryon s_e in units of Boltzmann's constant k is

$$s_e = Y_e \frac{S_e}{Nk} = Y_e \left[\frac{5}{3} \frac{F_{3/2}(\xi)}{F_{1/2}(\xi)} - \xi \right], \quad \xi = \frac{W_e^F}{kT}. \quad (6)$$

Here N is the number of baryons per unit volume, Y_e is the number of electrons per baryon, ξ is the total electron degeneracy parameter (i.e., W_e^F is the total electron Fermi energy, including both rest mass and kinetic energy), and the F 's are the standard nonrelativistic Fermi integrals defined in Chiu (1968). The degenerate limit, $\xi \gg 1$, is not relevant to the non-degenerate supermassive stars. The nondegenerate limit of equation (7) is

$$s_e \approx Y_e \left\{ \frac{5}{2} + \ln \left[\left(\frac{m_e kT}{2\pi\hbar^2} \right)^{3/2} \frac{g}{n_e} \right] \right\}, \quad (7)$$

where m_e is the mass of the electron, $g = 2J + 1 = 2$ for the electron, and $n_e = \rho N_A Y_e$ is the number of electrons per unit volume. This expression can be generalized for the ions and free nucleons to

$$S_i \approx \frac{X_i}{A_i} \left\{ 29.205 + \ln \left[\frac{g_i A_i^{5/2}}{\rho X_i} (kT)^{3/2} \right] \right\}, \quad (8)$$

where X_i is the mass fraction of Maxwell-Boltzmann species i , A_i is the atomic mass in amu, ρ is the density in units of g cm^{-3} , kT is the temperature in MeV, and g_i is the spin degeneracy factor at low enough temperature.

For relativistic spin $\frac{1}{2}$ particles the general expression for entropy per baryon is

$$s_e = Y_e \frac{S_e}{Nk} = Y_e \left[\frac{4}{3} \frac{F_3(\xi)}{F_2(\xi)} - \xi \right], \quad (9)$$

where the notation is as in equation (7) and where the F 's are now the relativistic Fermi integrals (Chiu 1968). The degenerate limit of this expression, $\xi \gg 1$, is again not of relevance for supermassive stars, but the nondegenerate limit will be of importance during the collapse phase of objects on their way into black holes and is given here as

$$s_e \approx \frac{1}{2} \frac{7\pi^2}{45} \left(\frac{kT}{\hbar c} \right)^3 \frac{1}{\rho N_A} \approx (1.667 \times 10^8) \frac{(kT)^3}{\rho}, \quad (10)$$

where we have assumed $kT \gg m_e c^2$ and the expression on the right is for kT in MeV and ρ in g cm^{-3} . An identical expression holds for positrons in this limit (equal numbers of electrons and positrons). The expression for photons is similar,

$$s_\gamma = \frac{4\pi^2}{45} \left(\frac{kT}{\hbar c} \right)^3 \frac{1}{\rho N_A} \approx (1.905 \times 10^8) \frac{(kT)^3}{\rho}, \quad (11)$$

where kT is in MeV and ρ in g cm^{-3} in the expression on the right.

For stars of mass $M \approx 10^5$ – $10^6 M_\odot$ the total entropy per baryon is $s_{\text{tot}} \approx 1000$, with s_γ making the dominant contribution. This contrasts markedly with typical main-sequence stars like the Sun where $s_{\text{tot}} \approx 10$ – 20 and where $s_\gamma \approx 10^{-3}$, or with white dwarfs or the cores of massive highly evolved stars where the entropy comes mostly from the electron gas and $s_{\text{tot}} \approx 1$. Very massive stars, in the 1000 – $2000 M_\odot$ range, have $s_{\text{tot}} \approx 100$ with similar entropy contributions from ions and photons (see Bond, Arnett, and Carr 1984). Just as the recognition of low entropy in supernova core collapse allows a simplified treatment of the equation of state (Bethe *et al.* 1979), the very high entropies due to photons encountered in a supermassive star allow the effects on the equation of state and the stability of the star due to the ions to be calculated perturbatively (see Shapiro and Teukolsky 1983).

The local adiabatic index in the limit of high entropy can be shown to be (Chandrasekhar 1939)

$$\Gamma_1 \approx \frac{4}{3} + \frac{\beta}{6} + O(\beta^2), \quad (12)$$

to first order in β . In other words, radiation-dominated stars are nearly $\Gamma = 4/3$ and thus “trembling on the verge of instability” as Fowler (1964) wrote. Stars with $\Gamma = 4/3$ have total energy zero, are in a state of neutral equilibrium, and have no natural length scale. This latter well-known property stems from the fact that in an index $n = 3$ polytropic configuration the expression for the mass has no dependence on central density. The mass is essentially the Jeans mass and will remain self-similar in density distribution through homologous expansion or contraction. Goldreich and Weber (1980) showed that a homologously collapsing solution can be found for the equations of motion for a $\Gamma = 4/3$, $n = 3$ configuration, as long

as the initial hydrostatic support pressure is reduced by no more than 3.2%. We will come back to this point later in examining the nonhomologous collapse of supermassive stars.

Since the adiabatic index of supermassive stars is so close to $\Gamma = 4/3$, small effects which are usually negligible in normal stellar evolution must be included to determine the stability properties of supermassive stars. These small perturbations include small amounts of rotation, electron-positron pair formation, the dissociation of heavy nuclei, and general relativity. Of these, the electron-positron pair instability, rotation, and general relativity are most relevant for determining the behavior of supermassive stars. In this paper we shall be restricting ourselves to nonrotating stars only. The electron-positron instability takes place in a restricted range of temperature and density where the energy in the photon gas, which is providing the support pressure, is drained into the creation of the rest mass of pairs. This rest mass energy provides no pressure and results in an instability. For stars in the mass range $M = 10^5$ – $10^6 M_\odot$, the principal subject of this paper, the pair transition takes place well after the collapse of the star has set in because of general relativity.

It is ironic that a star whose structure is determined nearly completely by Newtonian gravitation should be unstable because of general relativity, a truly minor perturbation on the gravitational force in the star (the Newtonian potential is $\phi/c^2 \ll 10^{-3}$). This instability in radiation dominated stars has its origin in the fact that Γ is nearly $4/3$. It was first suggested by Chandrasekhar (1964) and Feynman (1963) and was first applied to stars by Hoyle and Fowler (1963) and Iben (1963). The usual treatment is to note that the condition for hydrostatic equilibrium can be expressed as a variational principle: the total energy of the star is an extremum. The total energy is a function of the mass of the star, the entropy, and the central density (if a polytropic run of density is assumed). Extremizing the energy then determines the equilibrium mass for a given entropy and central density or, equivalently, the equilibrium energy for a given mass, central density, and entropy. If the star is started at low enough central density, the equilibrium energy will be nearly zero because of Γ_1 being close to $4/3$ throughout the star. The star will quasi-statically contract, radiating away entropy and increasing the central density while the equilibrium energy decreases. However, general relativistic corrections to gravity will cause the equilibrium energy to have a minimum, so that beyond a critical density, ρ_{crit} , energy must be added to achieve hydrostatic equilibrium. The supermassive star, shining at the Eddington luminosity, quasi-statically radiates away its entropy and shrinks to the point where the central density reaches the critical density and instability sets in. Here the equilibrium energy is stationary, and hence the total energy of the system has a second derivative of zero, indicating instability. When the star reaches this point it becomes dynamically unstable and begins to collapse. Iben (1963) and Fowler (1964) pointed out that stars in the mass range 10^5 – $10^7 M_\odot$ reach this instability point before the onset of nuclear reactions, so that the central question of the evolution of supermassive stars becomes whether or not nuclear energy liberated through hydrogen burning can be added fast enough to maintain or exceed hydrostatic equilibrium and cause a thermonuclear explosion.

The analysis of stability outlined above has been carried out by many authors, and here we simply summarize their results. We recommended the reviews by Shapiro and Teukolsky (1983), Fowler (1964), and Chandrasekhar (1964) as being the

most complete discussions of the general relativistic instability calculations discussed above.

The critical central density for a radiation dominated, high entropy, index $n = 3$ polytrope is

$$\rho_{\text{crit}} \approx 1.994 \times 10^{18} \left(\frac{0.5}{\mu} \right)^3 \left(\frac{M_{\odot}}{M} \right)^{7/2} \text{ g cm}^{-3}, \quad (13)$$

where μ is the mean molecular weight (0.5 for pure hydrogen) and M is the mass. for a mass of $M = 5 \times 10^5 M_{\odot}$, typical of those masses considered in the numerical calculations presented in this paper, the critical central density is $\rho_{\text{crit}} \approx 0.02 \text{ g cm}^{-3}$. Since supermassive stars are nearly index $n = 3$ polytropes we can use the polytropic relations to express the stability/instability conditions in other ways. From Chandrasekhar (1964), instability sets in when the radius of the star R is less than a critical radius R_{crit} ,

$$R_{\text{crit}} \approx \frac{6.8}{\beta} \left(\frac{2GM}{c^2} \right). \quad (14)$$

Another way to express the stability criterion is to give a critical adiabatic index Γ_{crit} , which the pressure averaged adiabatic index Γ_1 must exceed to ensure stability. The value of Γ_{crit} is clearly $4/3$ for a Newtonian star, but in the presence of a small general relativistic correction it becomes

$$\Gamma_{\text{crit}} \approx \frac{4}{3} + 1.12 \left(\frac{2GM}{Rc^2} \right). \quad (15)$$

This expression is to be compared to Γ_1 in equation (13) to determine stability. Note that for a star of mass $M = 5 \times 10^5 M_{\odot}$ composed of pure hydrogen at the instability radius, equations (13) and (16) yield $\Gamma_1 \approx \Gamma_{\text{crit}} \approx 1.3350$. As we shall see in the next section, the numerical results reproduce the expected behavior of those parameters around the instability point quite well thus giving one faith that the instability we are studying is a physical, not numerical one.

IV. NUMERICAL CALCULATIONS

We have computed a number of supermassive star models, each starting from a hydrostatic configuration well outside its instability radius and evolved to the endpoint of its evolution: collapse or explosion. The initial masses and compositions of these models were selected from a grid of masses between $10^5 M_{\odot}$ and $10^6 M_{\odot}$ and metallicities between $Z = 0$ and $Z = 10^{-2}$ by mass fraction. The KEPLER stellar evolution, hydrodynamics code, as described in Weaver, Zimmerman, and Woosley (1978), has been employed in these calculations, with modification to include a post-Newtonian approximation to general relativistic gravity and the nuclear reactions of the rp-process.

The KEPLER computer code is an implicit hydrodynamics code which integrates the conservation equations for mass, momentum, and energy and assumes spherical symmetry; in other words, no rotation or magnetic fields are considered unless these are introduced in a perturbative, one-dimensional manner. The Euler equation has been modified by a post-Newtonian gravitation approximation and in Lagrangian coordinates becomes

$$\frac{dv}{dt} = 4\pi r^2 \frac{\partial P}{\partial m_r} - \frac{G_{\text{rel}} m_r}{r^2} + \frac{4\pi}{r} \frac{\partial Q}{\partial m_r}, \quad (16)$$

where v is the velocity, d/dt is the covariant derivative follow-

ing the motion, m_r is the mass interior to radius r , P the pressure, $Q \equiv 4/3 \eta_v r^4 (\partial/\partial r)(v/r)$ with η_v the artificial viscosity described in Weaver, Zimmerman, and Woosley (1978) (see their eq. [3]) and G_{rel} is a post-Newtonian gravitational coupling constant given by

$$G_{\text{rel}} \equiv G \left(1 + \frac{P}{\rho c^2} + \frac{2GM}{rc^2} + \frac{4\pi P r^3}{m_r c^2} \right), \quad (17)$$

where G is the Newtonian gravitational coupling constant, ρ the density, and c the velocity of light. This characterization of the post-Newtonian approximation in terms of an amplified gravitational coupling constant goes back to discussions in Iben (1963) and Hoyle and Fowler (1963). It is merely a formal representation of the important first order post-Newtonian corrections to the Newtonian gravitational force. These corrections are included directly in equation (16), which is solved implicitly. Note that two correction terms include the pressure and, therefore, some $\rho + P$ corrections for the energy density in radiation. The two post-Newtonian terms involving pressure are generally small compared to the $2GM/rc^2$ term, except near the center of the star where the pressure is maximal and the mass and radius are approaching zero. The energy equation is the same as that in Weaver, Zimmerman, and Woosley (1978) repeated here for clarity,

$$\frac{du}{dt} = -4\pi p \frac{\partial}{\partial m_r} (vr^2) + 4\pi Q \frac{\partial}{\partial m_r} \left(\frac{v}{r} \right) - \frac{\partial L}{\partial m} + \epsilon, \quad (18)$$

where u is the internal energy per unit mass, L the luminosity through radius r , and ϵ the local energy generation rate per unit mass. Nuclear energy generation and neutrino losses appear in ϵ , while pdV work appears in the first term on the right in equation (18). The second term on the right represents heating due to viscous stress and is small in the present calculations since shock waves never develop.

Convection is included in the usual mixing length formulation but is implemented with a time-dependent treatment. The mixing of different compositions in a convective region is accomplished by explicitly solving the time-dependent diffusion equation. This assures that there are no gross inconsistencies when nuclear burning times are comparable to convective mixing times. Where the adiabatic index is close to $\Gamma \approx 4/3$ and where radiation dominates the pressure, inertial terms associated with the acceleration and deceleration of convective cells may be important in the dynamics of supermassive stars. Such effects have been neglected here (but see Arnett and Fuller 1985) since the models are convective from the onset of the calculations.

The time scale associated with hydrodynamic processes in radiation-dominated stars is (Fowler and Vogl 1964)

$$\tau_{\text{HD}} \equiv \frac{1}{(24\pi G \rho)^{1/2}} \approx 2 \times 10^{-6} \left(\frac{M}{M_{\odot}} \right)^{7/4} \text{ s}. \quad (19)$$

In order to see a hydrostatic evolution phase, this time scale must be shorter than the modified Kelvin-Helmholtz or thermal time given by

$$\tau_{\text{KH}} \approx \frac{|E_{\text{min}}|}{L_{\text{Ed}}} \approx 3 \times 10^{16} \left(\frac{M}{M_{\odot}} \right)^{-1} \text{ s}, \quad (20)$$

where L_{Ed} is the Eddington luminosity and E_{min} is the absolute value of the total energy of the star at the relativistic or electron-positron pair instability point (Shapiro and Teu-

kolsky 1983). The hydrodynamic time scale is indeed shorter than the modified Kelvin-Helmholtz time for radiation dominated stars of mass $M \lesssim 10^8 M_\odot$, and thus it makes sense to treat such stars with a hydrodynamic stellar evolution code. In addition to these time scales we must ask what the thermal relaxation or radiative time scale is and compare this to the evolutionary time. For all the supermassive star models considered here there was adequate time for thermal relaxation to take place.

The opacity of the material in supermassive stars is predominantly due to electron scattering. However, the temperatures in the core can become high enough that the Klein-Nishina correction must be included for the scattering cross section (Weaver, Zimmerman, and Woosley 1978),

$$\sigma_K \approx \sigma_T [1 + 0.027kT - 4.88(kT)^2 \times 10^{-5}]^{-1}, \quad (21)$$

where kT is in keV and where σ_T is the Thompson scattering cross section. At high temperature the Klein-Nishina cross section is reduced over that of the Thompson cross section with the result that the local Eddington luminosity is increased. This may result in mass loss on a radiative time scale if the convective energy flux is not too much larger than the radiative energy flux, but this question was not pursued in this work.

Hydrogen burning is, of course, the most important nuclear energy source for supermassive stars. At temperatures less than $T \approx 5 \times 10^8$ K hydrogen burns on the standard β -limited CNO cycle, where the rate of burning and energy generation is limited by the two positron decays: $^{14}\text{O}(e^+ \nu)^{14}\text{N}$ lifetime 102 s, and $^{15}\text{O}(e^+ \nu)^{15}\text{N}$ lifetime 176 s (see Fowler 1965) for an assumed density of 100 g cm^{-3} .

At temperatures greater than $T \approx 5 \times 10^8$ K Wallace and Woosley (1981) showed that leakage out of the β -limited CNO cycle can be substantial because the $^{15}\text{O}(\alpha, \gamma)^{19}\text{Ne}$ reaction. Once out of the cycle, the flow consists of radiative proton captures and positron decays building up toward the iron peak: the rp-process. Wallace and Woosley (1981) showed that the rp-process can result in substantial increases in the hydrogen burning rate, with energy generation rates 200 or 300 times faster than the β -limited CNO cycle would give at the same temperature. The nucleosynthetic yields from material experiencing hot hydrogen burning on the rp-process consists of substantial quantities of intermediate mass nuclei. This is in contrast to the nucleosynthesis associated with the β -limited CNO cycle: essentially helium.

The rp-process has been included in these evolution/hydrodynamic calculations through a 10 isotope network (APPROX; Wallace and Woosley 1981) which suffices to mock-up the energy generation rate, and CNO cycle break-out characteristics of the rp-process. As we shall see, nonrotating supermassive stars do not explode on the rp-process, no matter what the initial metallicity, and thus nucleosynthesis due to the rp-process is not an important issue here.

We have started the KEPLER evolution calculations with a supermassive star initial model in hydrostatic equilibrium well outside the instability radius. For instance, the $M = 5 \times 10^5 M_\odot$ model was started with a central density of $\rho_c = 10^{-6} \text{ g cm}^{-3}$. In this configuration the star is very nearly an index $n = 3$ polytrope, stable with respect to general relativity. The evolution of this star consists of quasi-static contraction to the instability point, where the central density is equal to the critical density given in equation (14), $\rho_{\text{crit}} \approx 0.02 \text{ g cm}^{-3}$, for $M = 5 \times 10^5 M_\odot$ and $X_H = 75\%$, $X_{\text{He}} = 25\%$.

The composition of each initial model was set during this quasi-static contraction phase before the onset of instability. Initial models with zero metallicity had $X_H = 75\%$ and $X_{\text{He}} = 25\%$. Stars with larger initial metallicities had roughly the same proportions of hydrogen and helium and up to 1% "metals" by mass. The "metals" were introduced by changing the abundance of ^{14}N . As soon as nuclear processing began, the relative proportions of carbon, nitrogen and oxygen were quickly brought to a redistributed equilibrium.

As the instability point was approached the stellar models began to oscillate because of small amounts of nuclear burning and temperature-dependent changes in the opacity (see eq. [21]). These oscillations were abetted as the restoring forces of pressure or gravity became ineffective near the instability point.

The supermassive star models exhibited dynamic instability due to general relativity at the critical central densities given by equation (13). For the $M = 5 \times 10^5 M_\odot$ star the instability takes place at the onset of hydrogen burning at a central temperature of $T_c = 5 \times 10^7$ K. Figure 1 shows the run of density, temperature, pressure, and radius as a function of Lagrangian mass coordinate for the $M = 5 \times 10^5 M_\odot$ star at the instability point. The luminosity of the star is dominated by photons here and is approximately Eddington, $L \approx 10^{44} \text{ ergs s}^{-1}$, while the radius is $R \approx 5 \times 10^{14} \text{ cm}$, and the effective surface temperature is $T_{\text{eff}} \approx 4.8 \times 10^4 \text{ K}$. These photospheric parameters are to be regarded as highly uncertain because mass loss has not been included in the calculation. There are 145 mass zones in the star at this point. The subsequent evolution of this star depends on the rate of rise of temperature and density and hence on the nuclear energy generation rate and on the rate at which infall kinetic energy builds up in this dynamically unstable phase.

V. RESULTS AND ANALYSIS

The quasi-static contraction to the general relativistic instability point takes a few thousand years for the supermassive stars considered in this paper. The Kelvin-Helmholtz time is

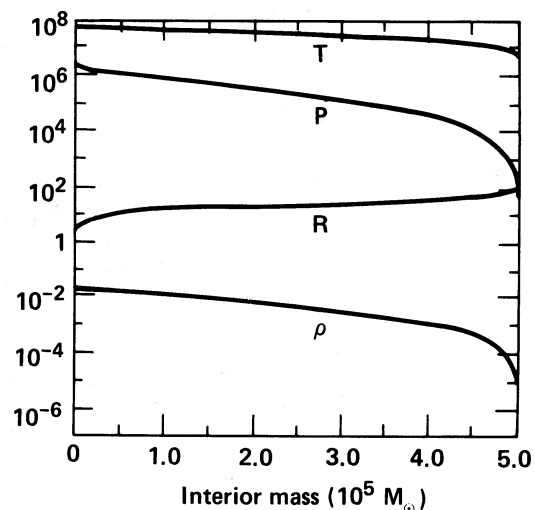


FIG. 1.—Run of temperature T (K), density ρ (g cm^{-3}), radius R (10^{12} cm), and pressure P ($10^{10} \text{ ergs cm}^{-3}$) with interior mass coordinate for the $5 \times 10^5 M_\odot$ star of metallicity $Z = 5 \times 10^{-3}$ at the general relativistic instability point. At this point the run of the radius and the thermodynamic variables is very closely that for an index $n = 3$ polytrope. There are 145 mass zones in this calculation.

TABLE 1
RESULTS

Initial Mass $M/10^5 M_\odot$ (1)	Initial Metallicity Z_{init} (2)	Fate (3)	Cumulative Time for $L > 10^{45} \text{ ergs s}^{-1a}$ (4)
1	0	Stable	...
5	0	Black hole	...
5	2×10^{-3}	Black hole	...
5	5×10^{-3}	$2.1 \times 10^{56} \text{ ergs}$ He: 0.249 \rightarrow 0.282	$> 3 \times 10^7 \text{ s}$
5	1×10^{-2}	$2 \times 10^{56} \text{ ergs}$ He: 0.247 \rightarrow 0.275	$> 2.6 \times 10^8 \text{ s}$
2.5	0	Black hole	...
10	0	Black hole	...
10	6×10^{-3}	Black hole	...
10	1×10^{-2}	$2.5 \times 10^{57} \text{ ergs}$ He: 0.25 \rightarrow 0.42	$> 10^8 \text{ s}$

^a The quantity L is the photon luminosity.

short compared to normal stars because the adiabatic index is so close to $4/3$. Once this dynamic instability occurs the battle between gravity and thermal pressure from nuclear energy is on. The outcome depends critically on whether hydrogen burning must wait on the $3\alpha \rightarrow {}^{12}\text{C}$ reaction to generate the requisite CNO contaminant.

The results of the present series of calculation are summarized in Table 1. Column (1) gives the initial mass in units of $10^5 M_\odot$. Column (2) gives the initial metallicity in nuclei heavier than helium by mass fraction. Column (3) gives the final fate of the star—either a black hole or an explosion. Calculations resulting in explosions have the explosion energy and the helium nucleosynthesis noted in the “Fate” column. Note that the $1 \times 10^5 M_\odot$ star burns hydrogen stably and had not suffered a post-Newtonian instability when the calculation was terminated. This star will burn hydrogen in a stable manner for $2 \times 10^6 \text{ yr}$ and will probably collapse on a pair or post-Newtonian instability at the onset of core carbon burning (Woosley and Weaver 1982) although the possibility of earlier collapse due to the post-Newtonian instability during helium burning will be investigated in Paper III of this series. The third column gives the cumulative time after the explosion for which the luminosity is greater than $10^{45} \text{ ergs s}^{-1}$.

The lowest metallicity for which an explosion takes place is $Z = 5 \times 10^{-3}$. Typical of the explosion results are those for the $M = 5 \times 10^5 M_\odot$ star with this critical metallicity. The configuration of the star at the instability point was given in the last section. At the instability point the star begins a rapid collapse wherein the central temperature and density quickly rise. Hydrogen burning at a very small rate has set in at the instability point since the central temperature at instability is just over the threshold value for hydrogen burning. As the temperature rises the nuclear energy generation rate increases dramatically. The central temperature and density of this model are plotted as a function of time in Figures 2 and 3, respectively, from the onset of collapse to well beyond the bounce. Figure 4 shows the total nuclear energy generation rate during this collapse and bounce.

The bounce of this model occurs when the pressure due to energy liberated by hydrogen burning balances gravity and makes up for infall kinetic energy. The central density and temperature at bounce are $\rho_c = 3.16 \text{ g cm}^{-3}$ and $T_c = 2.6 \times 10^8 \text{ K}$, respectively. The temperature is too low to affect

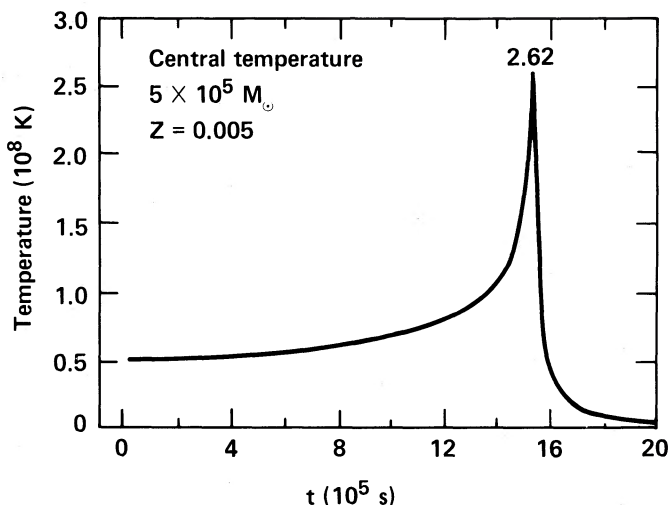


FIG. 2.—The history of the central temperature in units of 10^8 K is plotted as a function of time, in units of 10^5 s , from the onset of instability. This is again for the $5 \times 10^5 M_\odot$ star with initial metallicity $Z = 5 \times 10^{-3}$. A snapshot of this star at the instability point is shown in Fig. 1. Note that the central temperature reaches a maximum of $T_c = 2.62 \times 10^8 \text{ K}$ at the “bounce,” or turnaround, point where the collapse is halted and becomes an explosion. This central temperature is well below the threshold temperature for breakout of the CNO cycle and initiation of the rp-process.

breakout of the β -limited CNO cycle, with the result that the explosion occurs entirely on the β -limited CNO cycle. The photon luminosity of the star at bounce is $L_\gamma \approx 1.0 \times 10^{45} \text{ ergs s}^{-1}$, while the neutrino luminosity, $L_\nu \approx 1.0 \times 10^{41} \text{ ergs s}^{-1}$, is negligible.

The internal energy, kinetic energy, and total energy (including gravitation) are given as a function of time through the collapse and bounce of this model in Figure 5. Note that for a Newtonian, radiation-dominated star the total internal and gravitational energy will be nearly equal and of opposite sign, so that the total energy will be nearly zero. At the instability point of this model the total internal energy is $4.1 \times 10^{57} \text{ ergs}$ while the total Newtonian gravitational energy is $-4.1 \times 10^{57} \text{ ergs}$. Once the dynamical instability takes place the total energy quickly rises as nuclear energy is released.

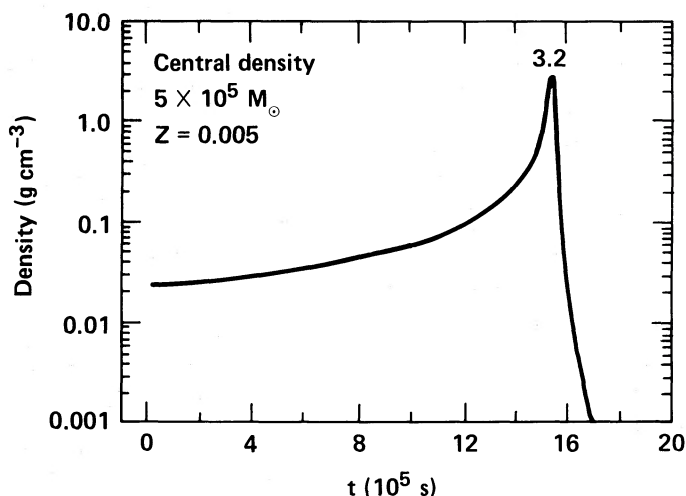


FIG. 3.—The history of the central density in units of g cm^{-3} as a function of time, in units of 10^5 s , from the onset of instability. This is for the same stellar model as in Figs. 1 and 2. The peak density at bounce is 3.2 g cm^{-3} .

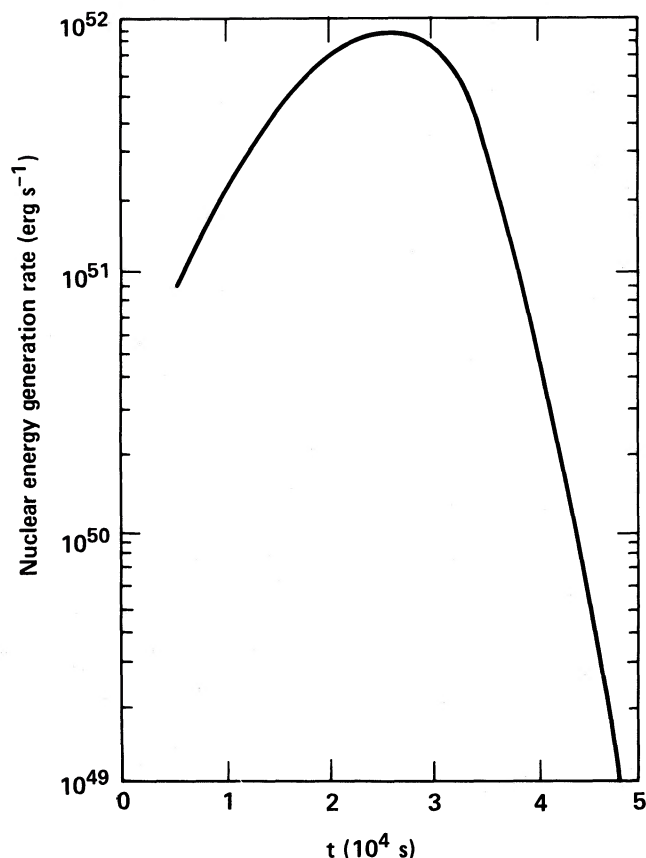


FIG. 4.—Nuclear energy generation rate (erg s^{-1}) is shown for the stellar model in the previous figures as a function of time (in units of 10^4 s) from the instability point. Nuclear energy generation is due entirely to hydrogen burning on the CNO cycle. The temperature during the collapse shown here is not high enough to trigger copious neutrino emission. The result is that the integrated thermal energy released by the hydrogen burning depicted here is $\sim 10^{56}$ ergs, which is eventually mostly converted to the kinetic energy of the explosion.

Note in Figure 5 that an increasing fraction of the total energy is kinetic energy after the bounce. Eventually the internal energy falls below the kinetic energy, and by 15 days after bounce nearly all of the energy of the explosion, 2.1×10^{56} ergs, is kinetic.

Since the explosion is a result of hydrogen burning on the CNO cycle the nucleosynthetic product is ^4He . The composition of this star long after bounce is plotted as a function of Lagrangian mass coordinate in Figure 6. The yield of ^4He by mass fraction of the star is somewhat less than that yielded in the explosion of the $M = 10^6 M_\odot$ star. This is because of the deeper gravitational potential well of the more massive star requiring a larger amount of hydrogen burning to achieve bounce and disruption.

The collapse, bounce, and expansion of our example star, and all the other models that gave explosions, were homologous. This homology is simply a consequence of the adiabatic index being nearly $4/3$ (and the polytropic index being $n = 3$). Such a configuration is scale invariant and is essentially right at the Jeans mass so that collapse or expansion will remain self-similar (Goldreich and Weber 1980). The final velocity for our example model is plotted in Figure 7 as a function of mass coordinate. Although it is not readily apparent from the figure, the velocity is very nearly proportional to the radius associated

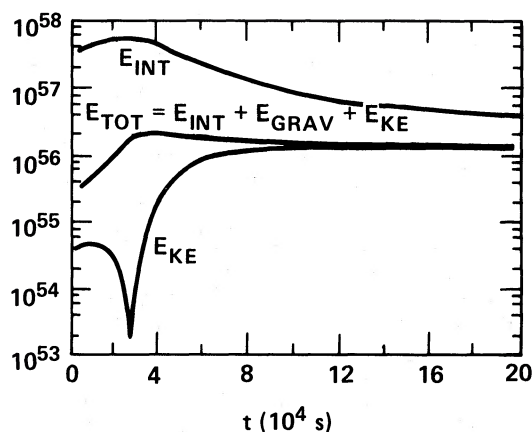


FIG. 5.—The kinetic energy, E_K , the internal energy, E_{int} , and the total energy E_{tot} (all measured in ergs) are plotted as a function of time (in units of 10^4 s) from the instability point for the same stellar model in the previous figures. Total energy, E_{tot} , includes the gravitational energy which is a negative quantity and is not separately plotted. The minimum in the kinetic energy curve corresponds to the bounce. The initial increase in E_{tot} is due to nuclear burning, and the slow decline in the total energy after the bounce is due to the escape of photon energy. The decline of the internal energy tracks the increase of kinetic energy after the bounce. At very late times after the bounce ($\sim 5 \times 10^5$ s) the internal energy curve falls well below the kinetic energy curve. Almost all of the extra internal energy generated by nuclear burning is eventually converted into the kinetic energy of expanding material.

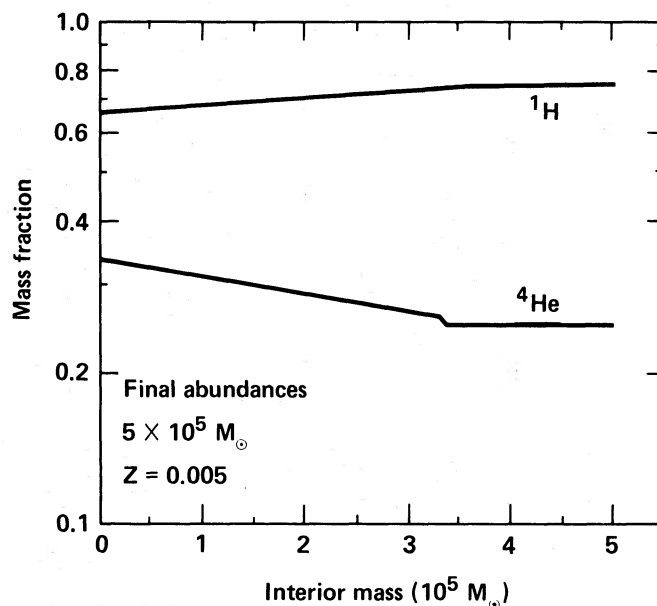


FIG. 6.—Final abundances (hydrogen and helium) resulting from the explosion of the $5 \times 10^5 M_\odot$ star with metallicity $Z = 5 \times 10^{-3}$ are shown as a function of internal mass coordinate in the star. Expansion of the star following the explosion is homologous, so that the density distribution remains self-similar and individual mass zones retain the abundances fixed in the explosion. Therefore, the inner mass zones in this stellar model show more processing of hydrogen into helium, while the outer zones show little or none. Mixing of the expanding material might result from Rayleigh-Taylor instabilities or other multidimensional effects at later times, but this calculation cannot reproduce those phenomena. Nearly $1.8 \times 10^4 M_\odot$ of ^4He is synthesized in this explosion.

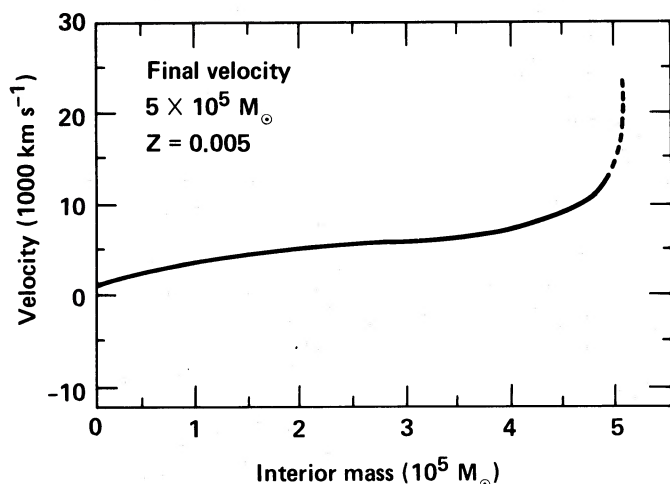


FIG. 7.—For the same stellar model as the previous figure we have plotted the final velocity (~ 5 days after bounce) for each mass zone as a function of internal mass coordinate. Although it is not evident from this figure, the expansion is very nearly homologous with the ratio of velocity to radius roughly constant for each mass zone. The dashed tail of the velocity curve near the surface of the star corresponds to mass zones which carry very little mass and which have been accelerated by radiation pressure throughout the evolutionary calculations of this model. Note that the bulk of stellar material, accelerated in the explosion, has a mean velocity of $\sim 5000 \text{ km s}^{-1}$, although the peak velocity is above $10,000 \text{ km s}^{-1}$.

with each mass zone (homology). The peak ejection velocity of the material in this explosion is $\sim v \approx 10,000\text{--}20,000 \text{ km s}^{-1}$. No shock wave developed in the calculation.

The light curve for this explosion is shown in Figure 8. The luminosity is roughly the constant Eddington luminosity

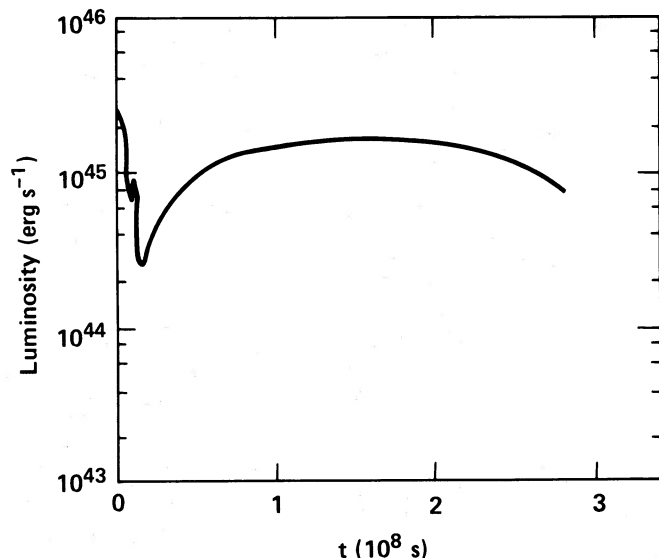


FIG. 8.—Light curve for the explosion of the same stellar model as in the previous figures is shown here. The photon luminosity in units erg s^{-1} is plotted as a function of time in units of 10^8 s from the bounce of the star. The luminosity starts out super-Eddington during the rapid expansion phase following the bounce, but falls rapidly as the energy of the explosion is converted to kinetic energy of ejected material. At $\sim 2 \times 10^7 \text{ s}$ after bounce a transparency wave moves back through the material as hydrogen begins to recombine. This causes a rise in luminosity to a “plateau” of $\sim 1 \times 10^{45} \text{ erg s}^{-1}$ where it remains for two to five years.

$\sim 10^{44} \text{ erg s}^{-1}$ through the quasi-static contraction phase. At later times the energy is, for the most part, siphoned into the kinetic energy of ejected material and the luminosity falls. Later still, the hydrogen begins to recombine, and a transparency wave moves back through the ejected material. This translates into a substantial rise in luminosity to a few times $10^{45} \text{ erg s}^{-1}$, where it remains for times of the order of two to five years, a phase that corresponds roughly to the “plateau” of an ordinary type II supernova (Woosley and Weaver 1982).

We now turn our attention to the failed explosions: those models that quasi-statically contracted to the instability point, became dynamically unstable, began collapsing, and ignited hydrogen burning but never generated adequate nuclear energy to halt the collapse. Typical of these failed-bounce calculations is the model with mass $M = 5 \times 10^5 M_{\odot}$ and zero initial metallicity. At the instability point the central density is $\rho_c \approx 0.02 \text{ g cm}^{-3}$, and central temperature $T_c \approx 4.8 \times 10^7 \text{ K}$, the stellar radius is $\sim R \approx 5 \times 10^{14} \text{ cm}$ with effective temperature $T_{\text{eff}} \approx 2.5 \times 10^4 \text{ K}$. Dynamical collapse ensues at this point with the central temperature and density rising quickly thereafter. Hydrogen burning at an appreciable rate awaits the production of a trace of catalyst ^{12}C from the 3α reaction.

By $t = 10^4 \text{ s}$ into the collapse the central temperature has risen to $T_c = 1 \times 10^9 \text{ K}$ and the central density to $\rho_c = 1000 \text{ g cm}^{-3}$. Under these conditions hydrogen is being burned very rapidly by the rp-process and, consequently, the energy generation rate is several orders of magnitude larger than that from CNO burning at the same temperature and density. An explosion does not result for two reasons: infall kinetic energy and neutrino energy losses.

An examination of the energy budget in this stellar model at the collapse conditions given above yields the result that the internal energy is $E_{\text{int}} = 4.1 \times 10^{58} \text{ ergs}$ while the Newtonian gravitational energy, $E_{\text{grav}} = -4.1 \times 10^{58} \text{ ergs}$, is roughly equal and opposite. The infall kinetic energy, however, is $E_{\text{kin}} = 2.1 \times 10^{57} \text{ ergs}$. While the star was dynamically collapsing, waiting for the 3α reaction to generate enough catalytic nuclei to burn hydrogen on the CNO cycle and by the rp-process, it built up a tremendous infall kinetic energy that cannot be matched by nuclear energy generation.

As the temperature rises to near $T = 10^9 \text{ K}$ electron-positron pairs are copiously produced. As a result, the neutrino energy-loss rates are substantial. For instance, in our example model described above, when the central density is $\rho_c = 1000 \text{ g cm}^{-3}$ and the central temperature is $T_c = 1.0 \times 10^9 \text{ K}$ the neutrino luminosity is $L_{\nu} = 1.2 \times 10^{52} \text{ erg s}^{-1}$, whereas the photon luminosity is $L_{\gamma} = 1.2 \times 10^{45} \text{ erg s}^{-1}$. The result is that all the extra thermal energy of the star, which is created by rapid hydrogen burning on the rp-process and by gravitational potential energy release in compressional heating, goes into neutrino energy losses. Wherever the temperature is high enough to burn hydrogen on the rp-process neutrino losses will become substantial.

The copious loss of thermal energy to neutrinos has another deleterious effect. It can be shown that the adiabatic constant in equation (2) is related to the entropy per baryon by

$$K \propto s_{\gamma}^{4/3}, \quad (22)$$

where we have used s_{γ} , the entropy per baryon from photons (eq. [11]) since radiation dominates the pressure and entropy. We have described two representative configurations in the $M = 5 \times 10^5 M_{\odot}$, $Z_{\text{init}} = 0$ calculation; one at the instability

point where $\rho_c = 0.02 \text{ g cm}^{-3}$ and $T_c = 4.8 \times 10^7$, and one at a point in the collapse after copious neutrino emission, $\rho_c = 1000 \text{ g cm}^{-3}$, $T_c = 1.0 \times 10^9$. If we call the set of conditions during collapse point 1 and those at the instability radius point 2, then the ratio of the adiabatic constants is given from equations (11) and (12) as

$$\frac{K_1}{K_2} = \left(\frac{\rho_2}{\rho_1}\right)^{4/3} \left(\frac{T_1}{T_2}\right)^4 \approx 0.1, \quad (23)$$

where K_1 and K_2 are the adiabatic constants at point 1 and 2 respectively. We see that neutrino losses have reduced the thermal energy to the extent that the adiabatic constant has been reduced by 90%. Neutrino losses are not the only source of thermal energy loss here. The creation of rest mass in electron-positron pairs from the radiation field has the same effect, since rest mass energy contributes nothing to pressure.

Goldreich and Weber (1980) showed that for a $\Gamma = 4/3$, $n = 3$ Newtonian polytrope, a homogeneously collapsing solution for the entire star can be found only as long as the adiabatic constant is reduced by no more than $\sim 3\%$. If the adiabatic constant is reduced by more than this during col-

lapse, then only a small "inner core" can collapse homogeneously (Brown, Bethe, and Baym 1982). In our collapsing supermassive star models, the collapse from the instability point is nearly homologous until the onset of copious pair production and neutrino losses; thereafter the collapse is non-homologous. Near the collapse point discussed above only the inner 10%–20% of the stellar mass is collapsing homogeneously.

In Figure 9 we have plotted the homology ratio, the ratio of velocity to radius, as a function of interior mass coordinate for two epochs in the collapse of the $5 \times 10^5 M_\odot$ star with metallicity $Z = 0$. The first epoch corresponds to a point early on in the collapse where the luminosity of the star is still dominated by photons and where $\sim 80\%$ – 90% of the mass of the star is collapsing homogeneously. The second epoch corresponds to a later point in the collapse of this star where the luminosity is dominated by neutrinos and where only 10%–20% of the star is collapsing homogeneously.

Although we cannot follow our collapses past the point where post-Newtonian gravity is adequate, we seen no way in which homology can be reestablished. This result is in contrast to other work on the collapse of supermassive stars, most

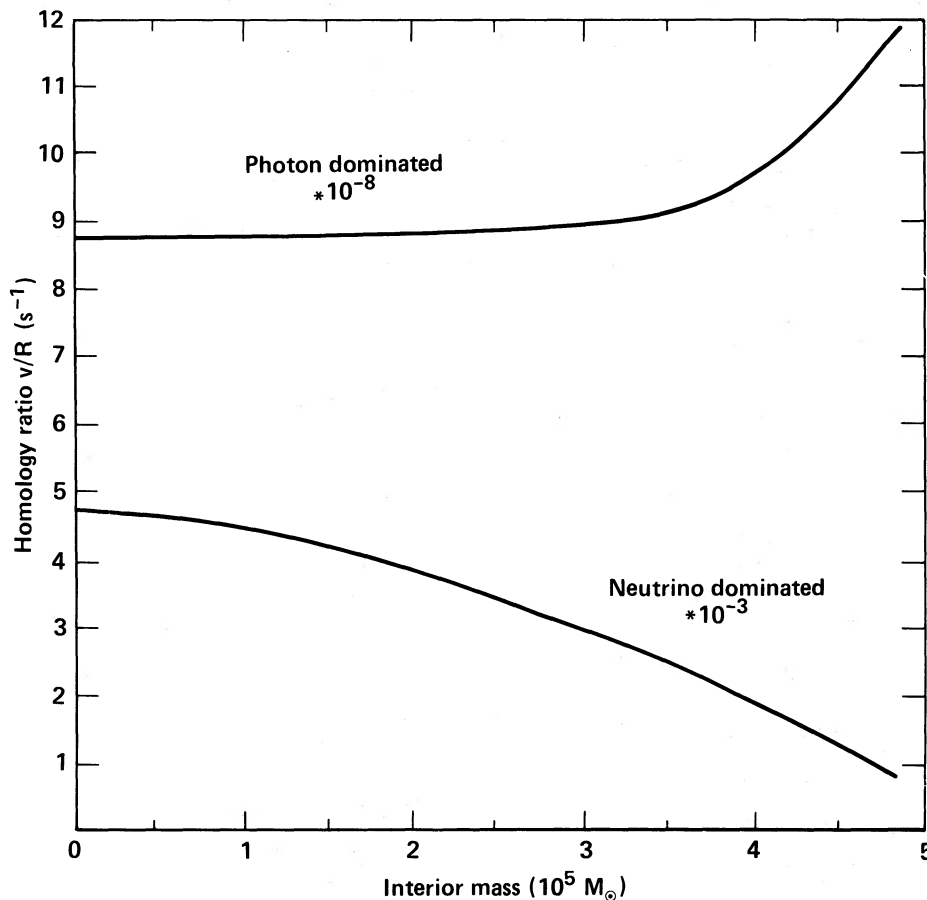


FIG. 9.—The ratio of the velocity to the radius (the homology ratio) is plotted for each mass zone as a function of interior mass coordinate for each of two stages in the collapse of a $5 \times 10^5 M_\odot$ star with initial metallicity $Z = 0$. Upper curve corresponds to the onset of collapse near the instability point. At this stage in the collapse the temperature is too low for substantial electron-positron pair formation and the neutrino luminosity is negligible compared to the photon luminosity. Homology corresponds to a roughly constant homology ratio so that the photon dominated stage is homogeneously collapsing (with deviations less than 10%) over 80%–90% of the mass of the star. The lower curve corresponds to a later stage in the collapse of the same stellar model. Here the central temperatures are well above 10^9 K , the rp-process is operating, and there is copious production of electron-positron pairs, with the result that the neutrino luminosity dominates the photon luminosity by many orders of magnitude. It can be seen that by this stage the homology ratio deviates significantly from a constant value over most of the star. Only the inner 10% of the star or less remains roughly homologous.

notably that of Shapiro and Teukolsky (1979). The latter calculation is fully relativistic, and hence more accurate where infall velocities are high and gravity is strong, and it assumes an index $n = 3$ polytrope and derives a homologous collapse. It would be enlightening if they could use our nonhomologous model with its exact equation of state and nuclear physics as input to the fully relativistic collapse calculation.

If homology is not reestablished, then the collapse of a supermassive star to a black hole is probably not so copious a source of long wavelength gravitational radiation as it was once thought to be (Thorne and Braginsky 1976; Thorne 1980; Shapiro and Teukolsky 1983). This follows from the fact that the power radiated in gravitational radiation is roughly proportional to the inverse fifth power of the collapse time scale: homology would send the most amount of stellar material through the event horizon in the shortest time. In contrast, the nonhomologous collapse found here would predict a much longer time scale for the nonhomologously collapsing material to flow into a trapped surface formed at the edge of the "inner-core."

VI. CONCLUSION

We have addressed here the classic problem of supermassive star evolution as posed by Hoyle and Fowler (1963), Iben (1963), and Fowler (1964): given that a nonrotating supermassive star has formed and quasi-statically contracted to its instability point, does the rapid nuclear burning that ensues following the general relativistic instability generate enough thermal energy to blow up the star? The answer is, of course, dependent on the initial mass and metallicity as Fricke (1973, 1974) discussed. Fricke (1973) concluded that a supermassive star of initial zero metallicity did not explode, but this result was cast in doubt by the elucidation of the rp-process and the application of it to supermassive stars (Fricke and Ober 1980). We have included in a hydrodynamic calculation the rp-process and a detailed equation of state with a correct treatment of electron-positron pair creation and neutrino losses. Our conclusions are roughly the same as Fricke (1973): zero initial metallicity, nonrotating, supermassive stars do not explode. Fricke (1973) made a survey of SMO evolution as a function of mass and mass fraction of elements in carbon and nitrogen. His result for the minimum metallicity for an explosion is $Z = 10^{-2}$. In our calculation the lowest metallicity for which there is an explosion is $Z = 5 \times 10^{-3}$. The explosion energies are in the range of 10^{56} – 10^{57} ergs in kinetic energy of ejected material for masses of 10^5 – $10^6 M_{\odot}$. These energies are large enough to account for some of the postulated energetics of QSO progenitors (Williams and Christiansen 1985).

When the rp-process does operate it has 200 or 300 times the

energy generation rate of the β -limited CNO cycle but it operates at such a high temperature that neutrino losses become dominant. Worse still, the infall kinetic energy built up as the star drops from the instability point until the 3α reaction has made a sufficient amount of CNO for hydrogen burning cannot be made up in subsequent nuclear reactions.

The high temperatures encountered in the collapse of supermassive stars translate into copious pair production and neutrino losses, which consequently produce a nonhomologous collapse. Supermassive stars collapsing nonhomologously are not likely to be quite so efficient sources of long wavelength gravitational radiation which they were once postulated to be.

The nucleosynthesis produced by a supermassive star exploding on the β -limited CNO process is a large amount of ^4He . There have been many attempts to produce the cosmological ^4He in an early generation of massive stars. We refer the reader to the paper of Carr, Bond, and Arnett (1981) for a discussion of these attempts. It has been suggested that deuterium may have been produced in supermassive stars (Woosley 1977). We find negligible production of deuterium because of the fragile nature of this nucleus and the high temperatures associated with the explosion of supermassive objects.

The helium mass fraction in both $5 \times 10^5 M_{\odot}$ explosions rises by 3% and in the $10^6 M_{\odot}$ explosion it rises by 16%. There are trace amounts of ^{15}N and ^7Li produced. One should keep in mind, however, that were it not for a near solar concentration of heavy elements these stars would never have exploded in the first place. Thus *nonrotating* supermassive stars heavier than $10^5 M_{\odot}$ had no part in producing pre-Galactic helium.

All of these conclusions are somewhat academic. Supermassive radiation dominated stars are very close to instability, and so tiny effects, like general relativity here, can have a profound effect on the stability and evolution of these stars. Foremost among the effects other than general relativity which can influence the evolution of these stars is a small amount of rotation. Rotation could provide a "spring" whereby the infall kinetic energy in the zero metallicity nonrotating, collapsing models is stored in rotation, the collapse is held up long enough for the 3α reaction to allow the rp-process to take over and generate enough thermal energy to affect an explosion. We shall return to this problem in a subsequent paper.

The authors gratefully acknowledge many stimulating and informative conversations with Willy Fowler on the subject of supermassive stars. This research has been supported by the National Science Foundation under grants AST 81-08509 A01 and AST 84-18185 and, at Livermore, by the Department of Energy under W-7405-EN6-48.

REFERENCES

- Appenzeller, I., and Fricke, K. 1972, *Astr. Ap.*, **21**, 285.
 Begelman, M. C., and Rees, M. J. 1978, *M.N.R.A.S.*, **185**, 847.
 Bethe, H. A., Brown, G. E., Applegate, J., and Lattimer, J. M. 1979, *Nucl. Phys.*, **A324**, 487.
 Bisnovaty-Kogan, G. S. 1968, *Soviet Astr.—AJ*, **12**, 58.
 Blandford, R. 1984, Caltech preprint GRP-021.
 Bond, J. R., Arnett, A. D., and Carr, B. J. 1984, *Ap. J.*, **280**, 825.
 Branch, D. 1984, in *Stellar Nucleosynthesis*, ed. C. Chiosi and A. Renzini (Dordrecht: Reidel), p. 19.
 Branch, D., and Greenstein, J. L. 1971, *Ap. J.*, **167**, 89.
 Brown, G. E., Bethe, H. A., and Baym, G. 1982, *Nucl. Phys.*, **A375**, 581.
 Carr, B. J., Bond, J. R., and Arnett, W. D. 1981, in *Proc. ESO Workshop on "The Most Massive Stars,"* ed. S. D'Odorico et al. (Garching: ESO), p. 315.
 Gassinelli, J. P., Mathis, J. S., and Savage, B. D. 1981, *Science*, **212**, 1497.
 Chandrasekhar, S. 1939, in *Introduction to the Study of Stellar Structure* (Chicago: University of Chicago Press), p. 57.
 ———. 1964, *Ap. J.*, **140**, 417.
 Chevalier, R. A. 1981, *Fund. Cosmic Phys.*, **7**, 1.
 Chiu, H. Y. 1968, *Stellar Physics*, Vol. 1 (Western, MA: Blaisdell).
 Dicke, R. H., and Peebles, P. J. E. 1968, *Ap. J.*, **154**, 891.
 Feynman, R. P. 1963, private communication to W. A. Fowler.
 Fowler, W. A. 1964, *Rev. Mod. Phys.*, **36**, 545, 1104E.
 ———. 1965, in *Quasi-Stellar Sources and Gravitational Collapse*, ed. I. Robinson, A. Schild, and E. L. Schucking (Chicago: University of Chicago Press), p. 51.
 ———. 1966, *Ap. J.*, **144**, 180.

- Fowler, W. A., and Hoyle, F. 1964, *Ap. J. Suppl.*, **9**, 201.
 Fowler, W. A., and Vogt, J. L. 1964, *Lecture in Theoretical Physics*, Vol. 6, (Boulder: University of Colorado Press), p. 379.
 Fricke, K. J. 1973, *Ap. J.*, **183**, 941.
 ———. 1974, *Ap. J.*, **189**, 535.
 Fricke, K. J., and Ober, W. 1980, *Ann. NY Acad. Sci.*, **336**, 399.
 Goldreich, P., and Weber, S. V. 1980, *Ap. J.*, **238**, 991.
 Hoyle, F., and Fowler, W. A. 1963, *M.N.R.A.S.*, **125**, 169.
 Iben, I. 1963, *Ap. J.*, **138**, 1090.
 Larson, R. B., and Starrfield, S. 1971, *Astr. Ap.*, **13**, 190.
 Ledoux, P. 1941, *Ap. J.*, **94**, 537.
 Lepp, S., and Shull, J. M. 1984, *Ap. J.*, **280**, 465.
 Norgaard, H., and Fricke, K. J. 1976, *Astr. Ap.*, **49**, 337.
 Ostriker, J. P., and Cowie, L. L. 1981, *Ap. J. (Letters)*, **243**, L127.
 Ozernoy, L. M., and Usov, V. V. 1971, *Ap. Space Sci.*, **13**, 3.
 Palla, F., Salpeter, E. E., and Stahler, S. W. 1983, *Ap. J.*, **271**, 632.
 Salpeter, E. E. 1964, *Ap. J.*, **140**, 796.
 Sanders, R. H. 1970, *Ap. J.*, **162**, 791.
 Schmidt, M. 1963, *Ap. J.*, **136**, 164.
 Shapiro, S. L., and Teukolsky, S. A. 1979, *Ap. J. (Letters)*, **234**, L177.
 ———. 1983, *Black Holes, White Dwarfs, and Neutron Stars* (New York: Wiley).
 Silk, J. 1977, *Ap. J.*, **211**, 638.
 Stoner, R., and Ptak, R. 1984, *Ap. J.*, **280**, 516.
 Talbot, R. J. 1971, *Ap. J.*, **165**, 121.
 Tohline, J. E. 1980, *Ap. J.*, **239**, 417.
 Thorne, K. S. 1980, *Rev. Mod. Phys.*, **52**, 285.
 Thorne, K. S., and Braginsky, V. B. 1976, *Ap. J. (Letters)*, **204**, L1.
 Truran, J. W., and Cameron, A. G. W. 1971, *Ap. Space Sci.*, **14**, 179.
 Utroban, V. P. 1984, *Ap. Space Sci.*, **98**, 115.
 Wagoner, R. V. 1969, *Ann. Rev. Astr. Ap.*, **7**, 553.
 Wallace, R. K., and Woosley, S. E. 1981, *Ap. J. Suppl.*, **45**, 389.
 Weaver, T. A., Zimmermann, G. B., and Woosley, S. E. 1978, *Ap. J.*, **225**, 1021.
 Wiescher, M. 1984, private communication.
 Williams, R., and Christiansen, D. 1985, preprint.
 Woosley, S. E. 1977, *Nature*, **269**, 42.
 Woosley, S. E., and Weaver, T. A. 1982, in *Supernovae*, ed. M. J. Rees and R. J. Stoneham (Dordrecht: Reidel), p. 79.
 Yoneyama, T. 1972, *Pub. Astr. Soc. Japan*, **24**, 87.
 Zeldovich, Ya. B., and Novikov, J. D. 1971, *Relativistic Astrophysics* (Chicago: University of Chicago Press).

G. M. FULLER: Institute for Nuclear Theory, Department of Physics, FM-15, University of Washington, Seattle, WA 98195

T. A. WEAVER: Special Studies Group and R-Program, Lawrence Livermore National Laboratory, Livermore, CA 94550

S. E. WOOSLEY: Board of Studies in Astronomy and Astrophysics, Lick Observatory, University of California, Santa Cruz, CA 95064